Journal of Applied Electrochemistry **34**: 815–822, 2004.

Pyrrole electropolymerization on copper and brass in a single-step process from aqueous solution

M. BAZZAOUI[1,2], J.I. MARTINS[1,2]*, E.A. BAZZAOUI[3], T.C. REIS[1,2] and L. MARTINS[2]
[1]*Departamento de Engenharia Química, Faculdade de Engenharia ,Universidade do Porto, rua Roberto Frias 4200-465 Porto, Portugal*
[2]*CISE, Departamento de Electrotecnica, Faculdade de Engenharia, Universidade do Porto, rua Roberto Frias 4200-465 Porto, Portugal*
[3]*Université Mohammed I^er^, Faculté des Sciences, Département de Chimie, 60000 Oujda, Morocco*
*(*author for correspondence: Departamento de Engenharia Química, Faculdade de Engenharia, Universidade do Porto, rua Roberto Frias 4200-465 Porto, Portugal; fax: +351-2-25081449; e-mail: jipm@fe.up.pt)*

Received 18 November 2002; accepted in revised form 8 March 2004

Key words: aqueous medium, brass electrode, copper electrode, corrosion, polypyrrole, sodium tartrate

Abstract

The electrosynthesis of polypyrrole (PPy) on copper and brass (Cu–Zn alloy) electrodes was performed by anodic oxidation of pyrrole in a sodium tartrate ($C_4H_4Na_2O_6$ 0.2 M) aqueous solution. The tartrate counter-ions slow the dissolution of the working electrode by leading to formation of a passivation layer on its surface, and pyrrole electropolymerization takes place. Strongly adherent and homogeneous polypyrrole films were electrodeposited on Cu and Cu–Zn alloy electrodes using different electrochemical techniques, such as potentiodynamic, galvanostatic and potentiostatic modes. The current densities of electropolymerization on brass are generally greater than those observed on copper. The corrosion behaviour of copper-coated electrodes, electrochemically modified by PPy films, was estimated by DC polarization and weight loss at different current densities in 0.1 M HCl solution. The synthesized polypyrrole films were characterised by several microscopic and spectroscopic techniques such as scanning electron microscopy, X-ray photo electron spectroscopy, Fourier transform infrared and Raman analysis.

Galvanostatically deposited PPy films are shown to be an alternative to common black-nickel or black-chromium as a decorative top-coating.

1. Introduction

The morphological and physical properties of conducting polymers have opened up a large field for specific industrial applications. At present, PPy can be considered an alternative to the black-nickel or black-chromium coatings on solar collectors or as a decorative top-coating.

A large number of optically selective surface coatings, from black paints to coated surfaces such as black-nickel [1] and black-chromium [2], have been developed in the past two decades. This black layer is deposited on a metal substrate surface such as aluminium, steel or copper, amongst other metals characterized by low emittance [3]. The deposits must be thermodynamically stable under all environmental conditions and strongly adherent to the substrate.

The electrodeposition of conducting polymers on oxidizable metals by electrochemical oxidation of the corresponding heterocyclic or aromatic monomers has been widely investigated [4–14]. Pyrrole is one of the most widely studied monomers considering its low oxidation potential (E_{ox} = 0.7 V vs SCE [6, 9]) and its high solubility in water (1.2 M [15]). In spite of these advantages, the electrosynthesis of polypyrrole on oxidizable metals is difficult. Indeed, the difference between the oxidation potential of pyrrole and the low oxidation potentials of oxidizable metals constitutes a serious obstacle to electropolymerization. Effectively, the dissolution of the working electrode is reached before the monomer oxidation and consequently the electropolymerization reaction is inhibited. Therefore, it is necessary to find new electrochemical conditions, such as solvents, supporting electrolytes and electrode treatments to slow down the dissolution rate of working electrodes without preventing electropolymerization. In this context, the first attempts on electrosynthesis of polypyrrole were carried out on noble metals, such as Pt and Au or inert materials such as glassy carbon [16–18].

The electropolymerization of pyrrole on oxidizable metals has been studied in different organic and aqueous media [4, 5, 19–23]. Generally, authors have used

electrodes that are chemically or electrochemically treated with aqueous solutions and thus capable of slowing down the metal dissolution by the formation of a passivation layer. Beck et al. showed that iron electrodes modified by a manganese oxide layer are needed to obtain adherent polypyrrole films in oxalic acid aqueous medium [8].

Recently, research has been reported on the aqueous electrodeposition of polypyrrole on zinc electrodes [13, 14, 22]. In this case, polypyrrole coatings were obtained in oxalate aqueous medium where the working electrode surfaces were modified by sulfide ions.

Pyrrole electropolymerization on Zn electrodes was also investigated in different organic media [10]. It was concluded that PPy film formation was only achieved in propylene carbonate with para-toluene sulfonate (Tos^-) anions as supporting electrolyte, and when the working electrode was treated with heteropolyanions such as $(H_2W_{18}O_{56}F_6)H_8 \cdot 9H_2O$, $P_2W_{18}O_{62}H_6 \cdot 9H_2O$ and $PW_{12}O_{40}H_3$.

In the present work, we describe a polypyrrole electrodeposition process on copper and brass with no preliminary chemical or electrochemical treatment of the electrode surfaces. The coatings obtained on copper and brass plates using different electrolysis techniques are homogeneous and strongly adherent, allowing application as a top-coating.

2. Experimental

Pyrrole monomer (Aldrich) was distilled under nitrogen, sodium tartrate ($C_4H_4Na_2O_6$, 99.5%) was purchased from Merck and used as received, while water was distilled twice before use.

The electrochemical experiments were performed in a one-compartment cell with three electrodes connected to an Autolab model PGSTAT20 potentiostat/galvanostat with pilot integration controlled by GPES 4.4 software. The working electrode was copper (99% of Cu) or brass (60% of Zn and 40% of Cu) in rectangular sheets (20×50 mm^2) or bars of 5 mm diameter. The Cu and Zn–Cu alloy electrodes were mechanically polished with abrasive paper (1200-grade) and rinsed in acetone before each experiment. A stainless-steel plate was used as auxiliary electrode. All potentials were measured versus an Ag/AgCl (KCl 0.1 M) reference electrode.

Scanning electron (SEM) micrographs were obtained on a JEOL JSM-6301F instrument.

X-ray photoelectron spectroscopy (XPS) analysis was carried out with a Vacuum Generators Microlab 310 F spectrometer equipped with MgK_α (1253.6 eV) operating at 200 W. The pressure in the analysis chamber ranged from 10^{-8} to 10^{-9} mbar and low intensity X-rays were focused on an area of about 40 mm^2 size. Calibration of spectra was performed by taking the C 1s electron peak ($E_b = 285$ eV) as internal reference.

Fourier transform infrared analysis in the reflection mode of the films electrodeposited on the working electrode was performed with a Nicolet 60 SX spectrometer.

The Raman spectra were carried out using a focused 514.5 nm laser beam of a Spectra Physics model 165 argon ion laser.

Adherence measurements were based on the standard Sellotape test, which consists in cutting the film into small squares, sticking on tape and then stripping it. The ratio between the number of remaining adherent film squares and their total number gives the percentage adherence.

Electrochemical corrosion measurements were performed at room temperature in 0.1 M HCl solution. The galvanostatic weight loss of the naked and PPy-coated bars electrodes was achieved in the range of 2–10 mA cm^{-2} applied current densities. A UNICAM Solar 969 Atomic Absorption Spectrophotometer was used for the determination of the metallic species concentrations in the solution.

3. Results and discussion

3.1. *Electrochemical behaviour of copper and brass in a 0.2 M sodium tartrate solution*

The electrochemical behaviour of copper and brass electrodes polarized in potentiodynamic mode between −1 and 2 V vs Ag/AgCl in a 0.2 M tartrate aqueous solution is shown in the Figure 1. In the case of Cu, an anodic wave is observed at about 1 V vs Ag/AgCl in the first potential sweep (Figure 1(a)). During the next successive sweeps the current density decreases with increasing cycle number, and two oxidation peaks appear at 0.3 and 1 V vs Ag/AgCl. The absence of the first peak on the voltammogram (Figure 1(c)) corresponding to a platinum electrode, polarized in the same electrolytic conditions, proves that, for copper, the peak comes from its oxidation, leading to the diffusion of a yellow-blue colour in the solution via the working electrode. The second peak at 1 V vs Ag/AgCl can be attributed to the adsorption and oxidation of tartrate ions on the working electrode surface by analogy with the electrochemical oxidation of tartaric acid on nickel [24].

The experiments performed on brass show an anodic peak at 0.25 V vs Ag/AgCl in the first cycle (Figure 1(b)), and, during the second potential sweep, a complex oxidation peak between −0.25 and 0.5 V vs Ag/AgCl. This last peak may be attributed to the heterogeneity of the alloy surface and probably corresponds to simultaneous oxidation of Zn and Cu. Similar behaviour has been reported by Kim et al. [25] for brass polarized in potassium hydroxide solution. The authors show that the oxidation may be interpreted as dissolution of zinc and copper. They concluded that the oxidation potential of zinc in brass is more positive than that of pure zinc.

A brown film was formed on copper and brass during the polarization process, which is probably related to copper-tartrate and copper/zinc-tartarate passivation films, respectively.

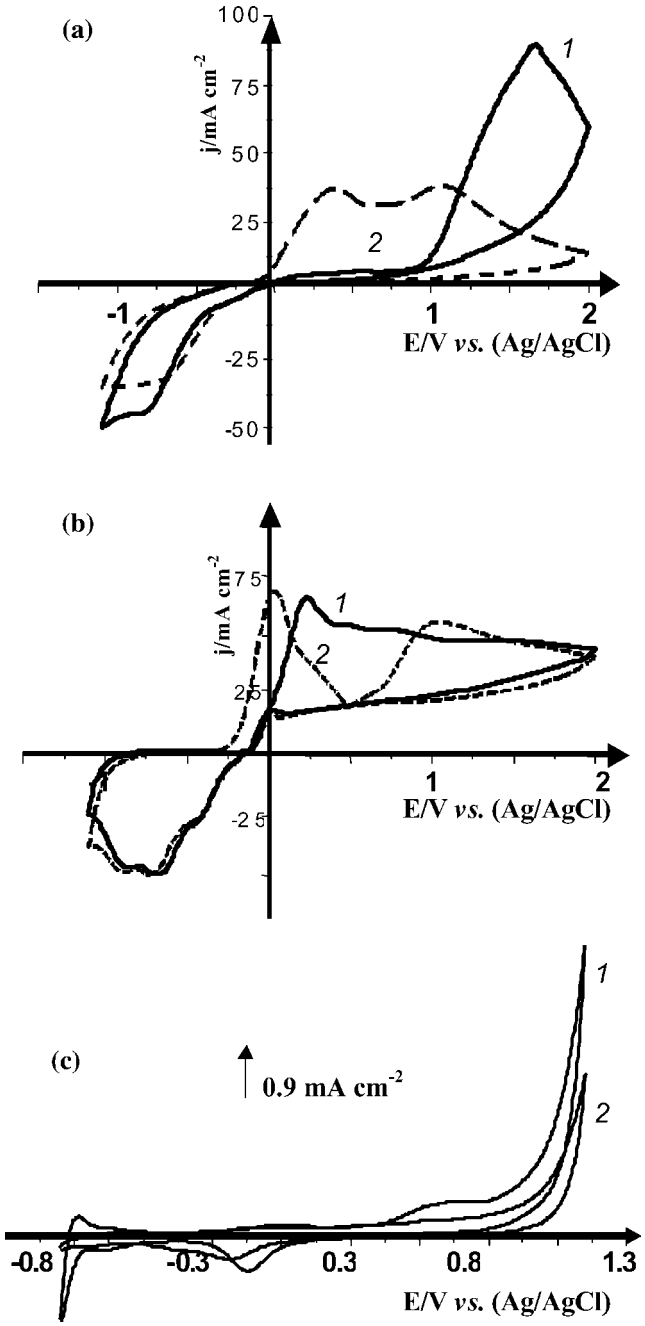

Fig. 1. Electrochemical behaviour of copper (a), brass (b) and platinum (c) electrodes in {H_2O + 0.2 M $C_4H_4Na_2O_6$} medium. Scan rate 100 mV s^{-1}.

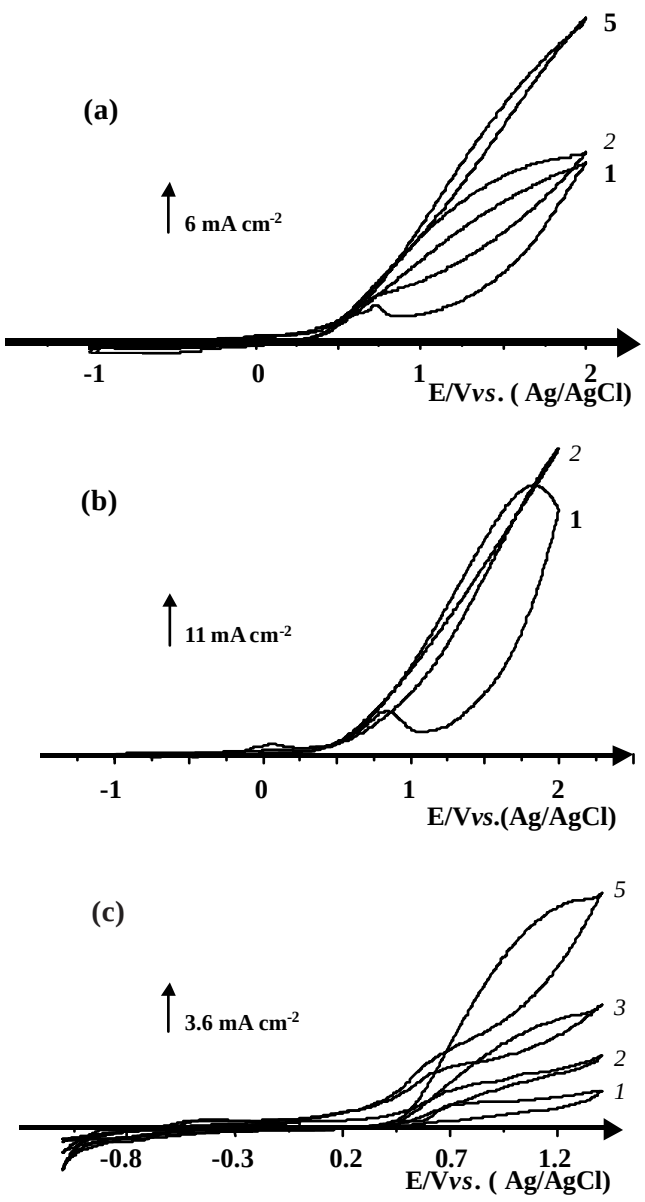

Fig. 2. Cyclic voltammograms of PPy film growth in {H_2O + 0.2 M $C_4H_4Na_2O_6$ + 0.5 M pyrrole} on copper (a), brass (b) and platinum (c) working electrodes. Scan rate 100 mV s^{-1}.

3.2. *Electropolymerization of pyrrole on copper and brass electrodes in a 0.2 M sodium tartrate and 0.5 M pyrrole aqueous solution*

The electropolymerization of pyrrole on copper and brass was performed in an aqueous solution of 0.2 M sodium tartrate and 0.5 M pyrrole, which is referred to in the text as the 'standard electrolyte'.

3.2.1. *Voltamperometric technique*

Figure 2 shows the voltamperometric curves of pyrrole electropolymerization on copper (a) and brass (b) electrodes obtained by sweeping the potential between −1 and 2 V vs Ag/AgCl at 100 mV s^{-1}. The behaviour of the potentodynamic curves is different from that observed without pyrrole. The oxidation peak of Cu and Cu–Zn alloy disappears and strong passivation of the working electrode occurs between −1 and 0.4 V vs Ag/AgCl. During the first potential sweep, an anodic wave is observed at 0.75 and 0.85 V vs Ag/AgCl on copper and brass respectively, which corresponds to the surface oxidation of pyrrole. The same peak is observed on platinum (Figure 2(c)), but only at 0.7 V vs Ag/AgCl. The potential drop is due to the presence of a passive layer of metal-tartrate. Effectively, on oxidizable metals the presence of the passivation layer constitutes a potential barrier to the electronic transfer necessary to achieve the oxidation potential of pyrrole.

During the next successive potential sweeps the oxidation wave of pyrrole occurs with an increased current

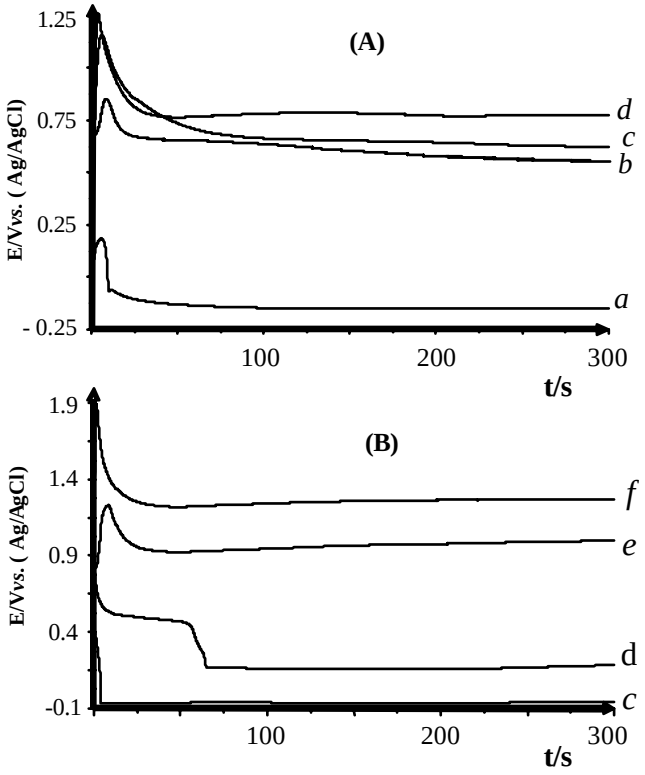

Fig. 3. Potential-time (*E–t*) curves for galvanostatic electropolymerization of pyrrole on copper (A) and brass (B) electrodes in {H_2O + 0.2 M $C_4H_4Na_2O_6$ + 0.5 M pyrrole} medium. Applied current densities: (a) 1 mA cm^{-2}, (b) 3 mA cm^{-2}, (c) 5 mA cm^{-2}, (d) 10 mA cm^{-2}, (e) 15 mA cm^{-2} and (f) 20 mA cm^{-2}.

density, and the thickness of PPy films grows regularly with the number of cycles. The *j–E* curves recorded in these cases become very close to those obtained on platinum (Figure 2(c)), and the PPy films on Cu and Cu–Zn alloy surfaces are very homogeneous and strongly adherent.

3.2.2. *Galvanostatic technique*

The electrodeposition of polypyrrole was carried out galvanostatically by applying different current densities ranging between 0.1 and 15 mA cm^{-2}. Figure 3 shows the influence of the applied current density and the nature of the working electrode metal on the behaviour of the potential–time curves.

In the case of Cu electrodes, at $j = 1$ mA cm^{-2} a rapid increase of the potential to 0.2 V vs Ag/AgCl is followed by a rapid decrease to a nil value of potential, and consequently no polymer grows on the electrode (Figure 3A). However, electropolymerization begins at 3 mA cm^{-2} and after 30 s the potential attains a value of 0.7 V vs Ag/AgCl which corresponds to the oxidation potential of pyrrole, and a thin homogeneous film of polypyrrole forms on the electrode. On the other hand, a polypyrrole coating only begins to form on Zn–Cu alloy at current densities equal to or greater than 15 mA cm^{-2} (Figure 3(B)).

Finally, it should be noted that high current densities are necessary to perform the electropolymerization reaction on brass. At least 15 mA cm^{-2} is necessary on Zn–Cu, while on Cu only 3 mA cm^{-2} is sufficient for PPy electrodeposition. This behaviour can be explained by the fact that on Cu almost all the total charge serves for electropolymerization, whereas on Zn–Cu alloys some of it is consumed in Zn dissolution.

Table 1. Potentiostatic electropolymerization of pyrrole on platinum, copper and brass in {0.2 M $C_4H_4Na_2O_6$ + 0.5 M pyrrole} aqueous medium

Applied E/V vs Ag/AgCl	Copper		Brass	
	Plateau j mA cm^{-2}	PPy formation*	Plateau j mA cm^{-2}	PPy formation*
0.6	6.0	n	9.3	n
0.8	14	y	11.4	y
1.0	–	y	17	y
1.2	33	y	24	y
1.4	37	y	32	y

*y: obtention of PPy film, n: no PPy film is obtained.

3.2.3. *Potentiostatic technique*

The electrosynthesis of PPy films on Cu and Zn–Cu alloy can also be performed in the potentiostatic mode, i.e. by imposing potential values (E_{imp}) that frame the known oxidation potential of the pyrrole. Table 1 summarises the threshold potentials for homogeneous PPy films growing on Cu and Zn–Cu alloy plates.

On copper and brass pyrrole electropolymerization takes place at a potential $\geqslant 0.8$ V vs Ag/AgCl (Figure 4(A) and (B)). For $E_{imp} < 0.8$ V, the potential is insufficient to allow a passage of current through the potential barrier constituted by the passive film. Thus, the current densities are weak and no PPy film is formed.

The polypyrrole films obtained on copper and brass under these conditions are homogeneous and adherent and their thicknesses depend on the applied potential as well as the polarization time. Increase in working electrode potential causes an increase in the current density plateau (j-t) and in the thickness of the coating.

3.3. *Characterization of the PPy coatings*

3.3.1. *X-ray photoelectron spectroscopy analysis*

The elemental composition and the doping rate of the PPy coating electrodeposited on copper electrodes after 10 potential sweeps using the standard electrolyte was investigated by XPS. These analyses reveal the presence of C, N and O related to the PPy film and the tartrate supporting electrolyte. The chemical assignments and derived elemental composition are summarized in Table 2.

The XPS signal of Cu 2p was not detected on the outer side of the PPy films, which clearly indicates their good homogeneity and compactness. A similar result was obtained by electropolymerization of pyrrole on iron in potassium nitrate solution [12].

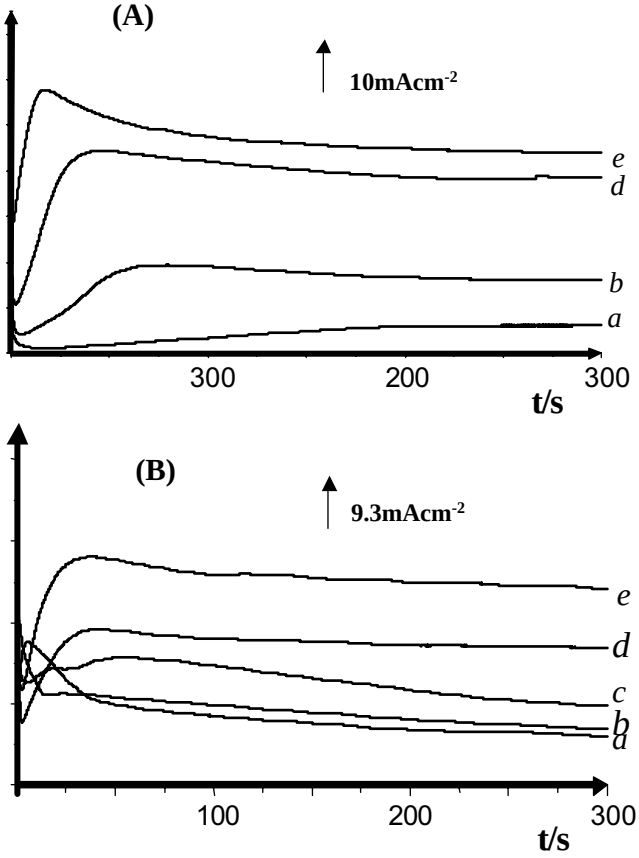

Fig. 4. Chronoamperometric curves obtained on copper (A) and brass (B) electrodes in {H_2O + 0.2 M $C_4H_4Na_2O_6$ + 0.5 M pyrrole} at 0.6 V (a), 0.8 V (b), 1.0 V (c), 1.2 V (d) and 1.4 V (e) vs Ag/AgCl.

XPS measurements were used to determine the doping rate (τ) within the polymer matrix. In our case, the doping level ranged from 27% to 33%. These values are similar to those reported for PPy electrosynthesized in organic media on noble electrodes, which generally do not exceed 30% [26–29].

3.3.2. *Vibrational analysis*

PPy films electrodeposited on copper in the standard electrolyte were analysed by infra-red and Raman spectroscopy. The results are shown in Table 3 and correspond to a standard PPy film.

Table 2. Results of qualitative XPS analysis of PPy films obtained in {H_2O + 0.2 M $C_4H_4Na_2O_6$ + 0.5 M pyrrole} medium on copper electrode

Signal	Binding energy/eV	Chemical structure
N 1s	398.0	=N—
	400.0	—NH—
	401.9	$C—N^+$
C 1s	285.0	C—C
	286.4	C—N, C—OH
	288.8	COO^-
O 1s	529	may be oxygen anion species
	531.3	C=O
	533.4	C—O—

3.3.3. *Morphological analysis*

PPy films electrosynthesized after 10 potential sweeps on copper and brass between −1.1 and 2.0 V vs Ag/AgCl at 100 mV s^{-1} in the standard electrolyte were analysed by scanning electron microscopy (SEM). The micrographs are shown in Figure 5. The PPy coatings are very homogeneous, compact and present a globular structure, finer in the case of copper (Figure 5(A)) in comparison to brass (Figure 5(B)). This difference of roughness is due to the composition of the underlying metal or alloy.

PPy films prepared galvanostatically on copper and brass were also investigated, and their adherence was estimated using a normalized sellotape test that gives a measure ranging from 0% to 100%.

Overall, the PPy films obtained at 15 mA cm^{-2} for 10 min on copper (Figure 5(C)) and brass (Figure 5(D)) are of uniform and compact nature. However, the structure of the PPy coating obtained on copper is cauliflower-like, while the PPy film electrosynthesized on Zn–Cu alloy plate is characterized by a globular texture with globules around 1 μm. Table 4 shows thicknesses evaluated by SEM analyses and current

Table 3. Wavenumbers and assignments of the Raman and IR bands of PPy films electrodeposited on copper electrodes

Experimental wavenumbers/cm^{-1}		Assignments	
IR	Raman	IR	Raman [30–34]
1703		Carboxylic groups or Carbonyl C=O groups [35, 36]	PPy overoxidation
	1583		C=C stretching vibration of pyrrole rings
1568		C=C stretching [37, 38]	
	1416		C—N groups vibration
1360		Stretching vibration of the pyrrole ring	
1285		Stretching vibration of the pyrrole ring	
1220		C—H in plane deformation [39]	
1045		N—H in plane deformation [40]	
	1050		C—H in plane deformation
964		C—H out-of-plane vibration	
	938		—C—H groups vibration
	860		—C—H out-plane deformations
792		C—H out-of-plane vibration	

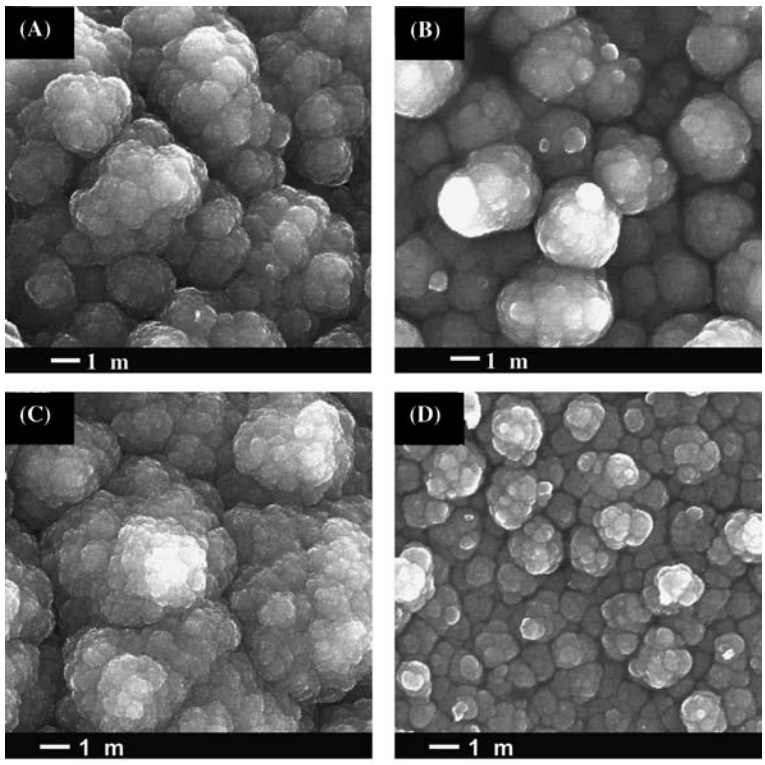

Fig. 5. SEM micrographs of PPy films electrosynthesized on copper (A and C) and brass (B and D) plates in {H_2O + 0.2 M $C_4H_4Na_2O_6$ + 0.5 M pyrrole} medium. A and B) scanning the potential 10 times between −1 and 2 V vs Ag/AgCl with 100 mV s^{-1} scan rate and (C and D) applied j=15 mA cm^{-2} current density during 10 min.

efficiencies of PPy films electrodeposited at different current densities for 10 min polarization on the two types of electrode.

Generally, it appears from these data that PPy films synthesized on copper are thicker than those on brass electrodes. This result is not surprising since it agrees with the columbic yield calculated for each case, and being higher for copper.

The oxidized PPy films adhere strongly to the brass and copper surfaces. According to the standard Sellotape test, the adherence was estimated at 100%, independent of the value of current density ranging between 3 and 25 mA cm^{-2}. This independence between adherence and the current density had not been observed previously [41], where the electropolymerization was performed in organic media and high-quality PPy films were obtained only at lower current densities.

Despite the strong adherence of the oxidized PPy films obtained in sodium tartrate, the polymer coatings became poorly adherent and were easily peeled off from the Cu and Zn–Cu when chemically reduced.

3.3.4. *Corrosion performance*

Figure 6 shows Tafel curves of naked and PPy-coated copper and brass bar electrodes polarized in 0.1 M HCl. The PPy films used in this test were electrodeposited by scanning the potential between −1 and 2 V vs Ag/AgCl for six cycles. The corrosion data, potential and current density, gathered in Table 5, reveal that the PPy coatings increased the corrosion potential and reduced the corrosion current density. Therefore, the corrosion rate of the metals has been decreased in comparison with those recorded for naked bar electrodes.

The electrochemical behaviour of the above electrodes in the same medium was investigated galvanostatically by analysing the ionic metallic content in the solution after 5 min under different applied current densities between 2 and 10 mA cm^{-2}. Figure 7 shows the varia-

Table 4. Thicknesses and coulombic yield of the PPy films electrosynthesized on copper and brass in {H_2O + 0.2 M $C_4H_4Na_2O_6$ + 0.5 M pyrrole} medium at various applied current densities with 10 min polarization time

Applied current density j mA cm^{-2}	Thickness of the PPy film and coulombic yield (γ)			
	PPy/Copper	γ/%	PPy/Brass	γ/%
5	8 μm	85	–	–
15	19 μm	89	14 μm	65
25	32 μm	89	26 μm	76

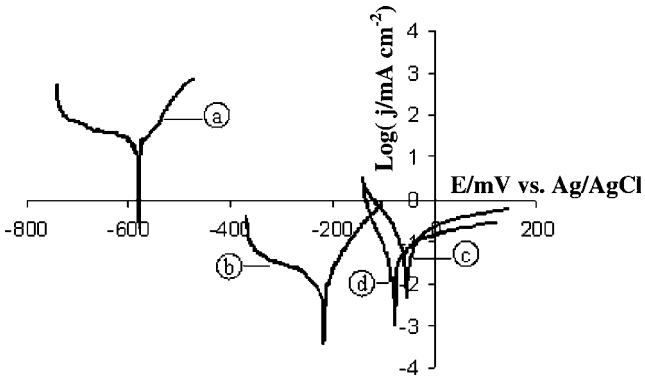

Fig. 6. DC polarization curves for uncoated brass (a) and copper (b), and PPy coated brass (c) and copper (d).

Table 5. Tafel results of bare or PPy-coated copper and brass electrodes polarized in 0.1 M HCl

Electrode	E_{corr}/mV	j_{corr}/mA cm^{-2}
Copper bare	−217.1	0.028
PPy/copper	−77.9	0.017
Brass bare	−580.5	18.560
PPy/brass	−56.8	0.100

tion of the Zn and Cu concentration diffused from PPy/brass and PPy/copper working electrodes with applied current density in comparison with those obtained for naked copper and brass electrodes. It is clear from this figure that the PPy coating is effective, retarding the working electrode dissolution.

In conclusion, the corrosion performance of PPy coatings, the Tafel and weight losses results show that PPy can act as an effective protective coating against corrosion of Cu and Cu–Zn alloy electrodes.

4. Conclusion

We have presented an electrosynthesis process producing homogeneous and strongly adherent polypyrrole films on copper and brass electrodes in sodium tartrate solutions. The electropolymerization was performed with no previous chemical or electrochemical passivation of the working electrode. Consequently, electrodeposition of polypyrrole was successfully achieved under different electrochemical techniques, such as potentiodynamic, galvanostatic and potentiostatic.

SEM, infra-red and Raman spectroscopy showed that the PPy films obtained have the same morphological and vibrational properties as those electrodeposited on Pt plates.

Acknowledgments

Funding from Fundação para a Ciência e a Tecnologia, POCTI/BPD/10873/2002, POCTI/CTM/41136/2001 and FEDER is gratefully acknowledged.

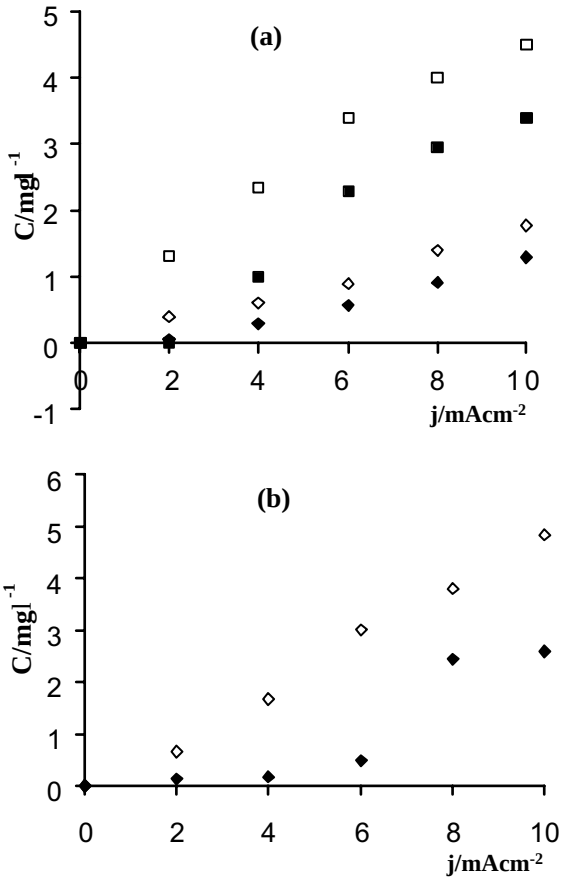

Fig. 7. The evolution of the concentration of Zn and Cu diffused from the working electrodes oxidation with the applied current densities during 5 minutes. (a) Brass electrode and (b) copper electrode. (□, ■) zinc species and (◇,◆) copper species. (□, ◇) bare electrode and (■, ◆) PPy coated electrode.

References

1. R.M. Khalil, A.G. Hamza, A.A. Ibrahim and A.A. El-Miligy, *Trans. Inst. Metal Finish.* **71** (1993) 99.
2. M.S.E. Abdo and T. Al-Sahhaf, *Plating Surf. Finish.* June (1998) 108.
3. J.F. Kreioder and F. Kreith, *Solar Heating and Cooling* (MgGraw-Hill, New York, 1975).
4. W. Janssen and F. Beck, *Polymer* **30** (1989) 353.
5. M. Schirmeisen and F. Beck, *J. Appl. Electrochem.* **19** (1989) 401.
6. C.A. Ferreira, S. Aeiyach, M. Delamar and P.C. Lacaze, *J. Electroanal. Chem.* **284** (1990) 351.
7. P. Hülser and F. Beck, *J. Appl. Electrochem.* **20** (1990) 596.
8. F. Beck and R. Michaelis, *J. Coatings Technol.* **64** (1992) 59.
9. C.A. Ferreira, S. Aeiyach, M. Delamar and P.C. Lacaze, *Surf. Interf. Anal.* **20** (1993) 749.
10. B. Zaïd, S. Aeiyach and P.C. Lacaze, *Synth. Met.* **65** (1994) 27.
11. F. Beck and P. Hüsler, *J. Electroanal. Chem.* **280** (1990) 159.
12. C.A. Ferreira, S. Aeiyach, J.J. Aaron and P.C. Lacaze, *Electrochim. Acta.* **41** (1996) 1801.
13. B. Zaïd, S. Aeiyach, H. Takenouti and P.C. Lacaze, *Electrochim. Acta.* **43** (1998) 2331.
14. C.A. Ferreira, B. Zaïd, S. Aeiyach and P.C. Lacaze *in* P.C. Lacaze (ed.), *Organic Coatings* (AIP Press, Woodbury, New York, 1996), pp. 159–165.
15. J.A. Dean (ed.), *Lange's Handbook of Chemistry* (Mc GRAW-HILL, New York, 1973).

16. T.A. Skotheim (ed.), *Handbook of Conducting Polymers* (Marcel Dekker, New York, 1986).
17. J.L. Brédas and R.S. Silkey (ed.), *Conjugated Polymers* (Kluwer, Dordrecht, 1991).
18. R.J. Waltman, J. Bargon and A.F. Diaz, *J. Phys.* Chem. **87** (1983) 1459.
19. F. Beck, P. Hülser and R. Michaelis, *Bull. Electrochem.* **8** (1992) 35.
20. C.A. Ferreira, S. Aeiyach, J.J. Aaron and P.C. Lacaze, *in* P.C. Lacaze (ed.), *Organic Coatings* (AIP Press, Woodbury, New York, 1996), pp. 153–158.
21. F. Beck, R. Michaelis, F. Schloten and B. Zinger, *Electrochim. Acta* **39** (1994) 229.
22. S. Aeiyach, B. Zaid and P.C. Lacaze, *Electrochim. Acta* **44** (1999) 2889.
23. J. Petitjean, S. Aeiyach, J.C. Lacroix and P.C. Lacaze, *J. Electroanal. Chem.* **478** (1999) 92.
24. M.J. Fish and D.F. Ollis, *J. Catal.* **50** (1977) 353.
25. B.S. Kim, T. Piao, S.N. Hoier and S.M. Park, *Corros. Sci.* **37** (1995) 557.
26. R.J. Waltman and J. Bargon, *Can. J. Chem.* **64** (1986) 76.
27. A.F. Diaz and J.C. Lacroix, *New J. Chem.* **12** (1988) 171.
28. A.O. Patil, A.J. Heeger and F. Wudl, *Chem. Rev.* **88** (1989) 183.
29. J. Roncali, A. Guy, M. Lemaire, R. Garreau and A.H. Huynh, *J. Electroanal. Chem.* **312** (1991) 277.
30. C.Q. Jin, X.G. Kong and X.J. Liu, *Synth. Met.* **55** (1993) 536.
31. M. Fukuyama, N. Nanai, T. Kojima, Y. Kudoh and S. Yoshimura, *Synth. Met.* **58** (1993) 367.
32. M.J. Hearn, I.W. Fletcher, S.P. Church and S.P. Armes, *Polymer* **34** (1993) 262.
33. C.M. Jenden, R.G. Davidson and T.G. Turner, *Polymer* **34** (1993) 1649.
34. G. Zerbi, M. Veronelli, S. Martina, A.D. Schluter and G. Wegner, *J. Chem. Phys.* **100** (1994) 978.
35. J.B. Schlenoff and H. Xu, *J. Electrochem. Soc.* **139** (1992) 2397.
36. F. Beck, P. Braun and M. Oberst, *Ber. Bunsenges. Phys. Chem.* **91** (1987) 967.
37. J.O. Iroh and G.A. Wood, *Compos. Part B.* **29B** (1998) 181.
38. J.W. Gargner and P.N. Bartlett, *Nanotechnology* **1** (1991) 19.
39. G.B. Street, T.C. Clarke, M. Krounbi, K.K. Kanazawa, V. Lee, P. Pfluger, J.C. Scott and G. Weiser, *Mol. Cryst. Liq. Cryst.* **83** (1982) 253.
40. K.M. Cheung, D. Bloor and G.C. Stevens, *Polymer* **29** (1988) 1709.
41. M. Bazzaoui, E.A. Bazzaoui, L. Martins and J.I. Martins, *Synth. Met.* **128** (2002) 103.